

Study on the Fatigue Experiment of TDCB Aluminum Foam Specimen Bonded with Adhesive

Sung-Soo Kim¹, Moon-Sik Han², Jae-Ung Cho^{3,#}, and Chong-Du Cho⁴

¹ Department of Mechanical Engineering, Graduate School, Kongju National University, 1223-24, Cheonan Daero, Seobuk-gu, Cheonan-si, Chungnam of Korea, 331-717

² Department of Mechanical and Automotive Engineering, Keimyung University, 2800 Dalgubeoldaero, Dalseo-Gu, Daegu, Korea, 704-701

³ Division of Mechanical & Automotive Engineering, Kongju National University, 1223-24, Cheonan Daero, Seobuk-gu, Cheonan-si, Chungnam of Korea, 331-717

⁴ Department of Mechanical Engineering, Inha University, 253, Yonghyeon-dong, Nam-gu, Incheon of Korea, 402-751

Corresponding Author / E-mail: jucho@kongju.ac.kr, TEL: +82-41-521-9271

KEYWORDS: Aluminum foam, Tapered double cantilever beam (TDCB), Fracture behavior, Adhesively bonded structures, Adhesive fracture energy, Critical fracture energy

In this study, TDCB specimen adhesively bonded with aluminum foam, which is the porous metallic material, is fabricated and critical fracture energy is measured in accordance with British standards (BS 7991 and ISO 11343). The specimens are classified by m value into 2, 2.5, 3, and 3.5 for comparison. " m refers to gradient which is expressed in the length (a) and (height) of the specimen. According to the result of reviewing axial displacement graph on crack length, displacement tends to increase in line with a growing crack, and the less the value of m , the higher the displacement. On the other hand, energy release rate tends to increase based on developing cracks, and the less the value of m , the higher the energy release rate. Based on correlations obtained in this study, the fracture behavior of bonding material is analyzed and aluminum foam material bonded using adhesive is applied to a composite structure in various fields, thereby analyzing the mechanical and fracture characteristics of the material.

Manuscript received: May 6, 2013 / Accepted: July 16, 2013

1. Introduction

Porous metallic material refers to the solid area in which pores or channels in certain shapes are distributed in regular or irregular patterns. Such porous material has the advantage of lightweight effect, superior impact resistance, and sound insulation performance and indicates similar stress-strain characteristics with the behavior of ductile material. It also has behavioral characteristics including smaller linear elasticity territory and larger plastic deformation.¹⁻⁴

Though the studies on the shock absorption of such a material with its great advantages have been underway, the study on bonding has been far behind.³ The importance of the fundamental study on fracture toughness data on glued joints, which is essential for safe bonding methods for adhesively bonded structures, should not be overlooked. Recently, evaluation methods applying fracture mechanics for strength evaluation of glued joints have been increasingly used. In case of the cracks developing in pure open mode (Mode I), inclined TDCB specimen has been used to identify the segregation among the layers of a composite material and adhesive failure characteristics to evaluate fracture toughness while the measurement method has long been developed as a standardized method.⁵⁻⁹

In this study, the TDCB specimen of an aluminum foam composite material is developed in accordance with British standards (BS 7991 and ISO 11343) with model I test being conducted. Based on the correlation obtained from this study, an analysis of fracture behavior is carried out and aluminum foam bonded using adhesive is applied to actual composite structures to analyze mechanical characteristics and fracture properties.¹⁰⁻¹⁵

2. Specimen

2.1 Appearance and dimension of specimen

TDCB specimen is developed based on BS and ISO requirements and Fig. 1 shows the structure of glued joints according to British Standards.

3M's spray 77 is used as bonding material. Fig. 2 shows the specimen and the dimension is indicated in mm. The specimens are categorized into four kinds with the m value of 2, 2.5, 3, and 3.5. m referring to the gradient of the specimen which is expressed in the function of the crack length (a) and height of the specimen (h). Fig. 3 indicates the dimension of the specimens depending on the m value.

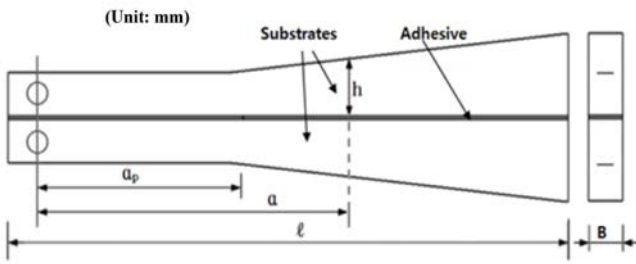


Fig. 1 British standard (BS)

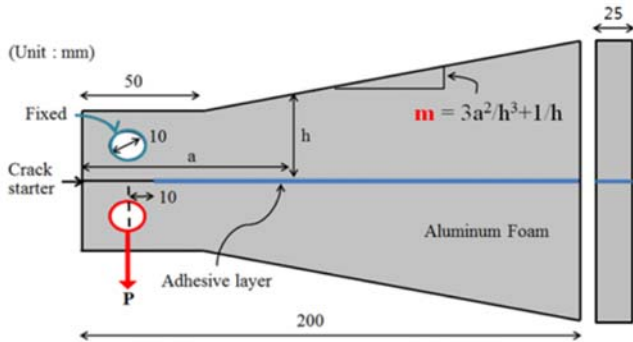


Fig. 2 Drawing of specimen

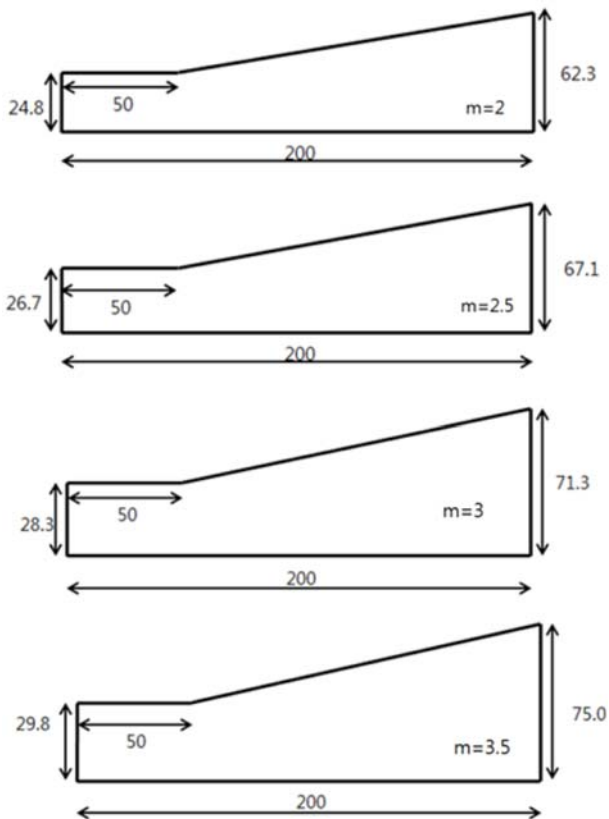


Fig. 3 Dimensions of specimens (unit: mm)

The specimens are bonded by applying adhesives on the surface of aluminum foam at 0.2 mm thickness and in 2 hours. Another 0.2 mm-thick layer of adhesive is applied before bonding two aluminum foams.

Table 1 Property of aluminum foam

Property	Value
Young's modulus (MPa)	2,374
Poisson's ratio	0.29
Density (kg/m ³)	400
Yield strength (MPa)	1.8
Shear strength (MPa)	0.92



Fig. 4 Experimental specimen

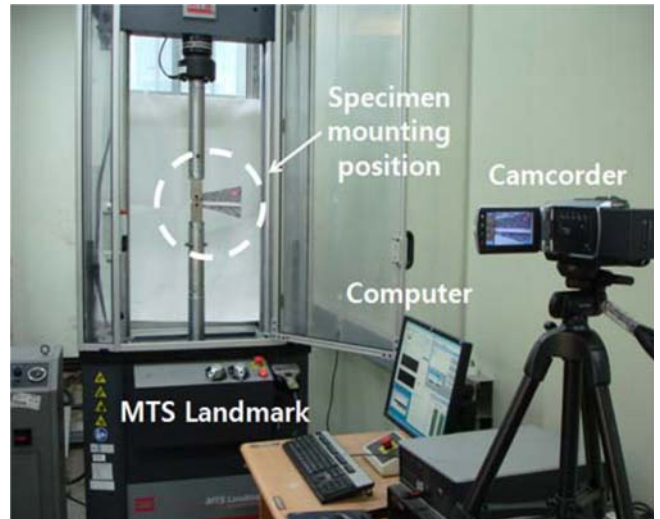


Fig. 5 Test device

The thickness of adhesive after bonding and compression is 0.3 mm. The properties of aluminum foam are indicated in Table 1.

Fig. 4 shows experimental specimen with the tape indicating the number to measure the length of crack. For more accurate test data, a number of specimens per case are produced by Foam Tech(Aluminum Foam Company, Korea) to measure the mean value for analysis.

2.2 Test device and setup

The MTS Landmark tester as seen in Fig. 5 is used for this study. The test's resulting data are produced using a computer and an experimental scene of each specimen is recorded using a camcorder.

The specimen is fixed to a jig connected to a load cell as seen in Fig. 6. The test is carried out by imposing 160 N of repeated load downward while the cycle of loading is set to 2 cycle/s.

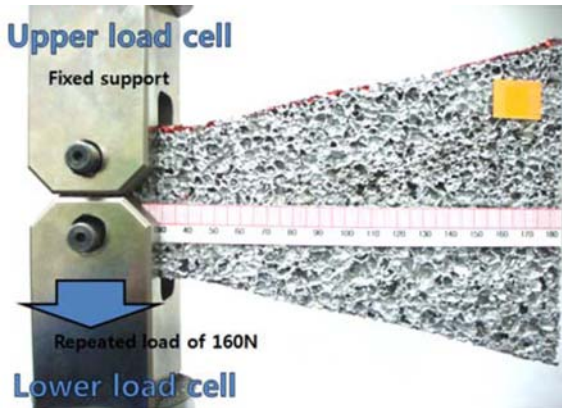


Fig. 6 Fatigue test setup

2.3 Critical fracture energy (G_{IC}) according to the corrected beam theory method

Critical fracture energy (G_{IC}) is calculated using Eq. 1 under Mode I load condition.¹¹

$$G_{IC} = \frac{P^2 dC}{2B da} \quad (1)$$

Compliance (C) is δP and B refers to the width of specimen while P and δ are applied load and displacement, respectively. C is calculated from bending and shearing strain as well as Eq. 2.

$$\frac{dC}{da} = \frac{8}{E_s B} \left(\frac{3a^2}{h^3} + \frac{1}{h} \right) \quad (2)$$

Compliance is linearly strained depending on crack length (a). Form factor of specimen (m) is constant while the height of specimen varies according to the shape, which leads to Eq. 3.

$$\frac{3a^2}{h^3} + \frac{1}{h} = m \quad (3)$$

A refers to crack length and h refers to the thickness of beam on the crack tip of a vertical line. E_s refers to the modulus of elasticity of a bonding surface; thus, critical fracture energy (G_{IC}) is calculated as indicated in Eq. 4 using Eqs. 1, 2, and 3.

$$G_{IC} = \frac{4P^2}{E_s B^2} \left(\frac{3a^2}{h^3} + \frac{1}{h} \right) = \frac{4P^2}{E_s B^2} \cdot m \quad (4)$$

In the existing SBT analysis, the compliance value of a specimen is calculated simply and accurately in general but no rotation or refraction on a crack tip is assumed to have existed. CBT analysis, however, considers the possible rotation on a crack tip. Should form factor of specimen (m) be irrespective of $1/h$ of revision to shearing, dC/da is calculated as Eq. 5.

$$\frac{dC}{da} = \frac{8m}{E_s B} \left[1 + 0.43 \left(\frac{3}{ma} \right)^{\frac{1}{3}} \right] \quad (5)$$

Thus Eq. 6 is developed using equations 1 and 5 and critical fracture energy (G_{IC}) under load condition Model I is calculated.

$$G_{IC} = \frac{4P^2 m}{E_s B^2} \left[1 + 0.43 \left(\frac{3}{ma} \right)^{\frac{1}{3}} \right] \quad (6)$$

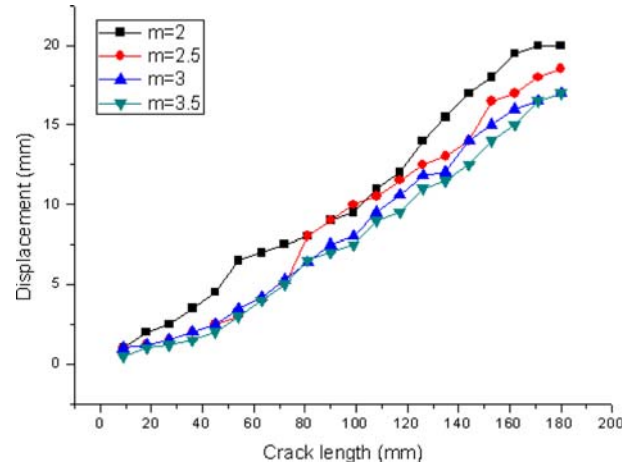


Fig. 7 Displacement deepening on crack length

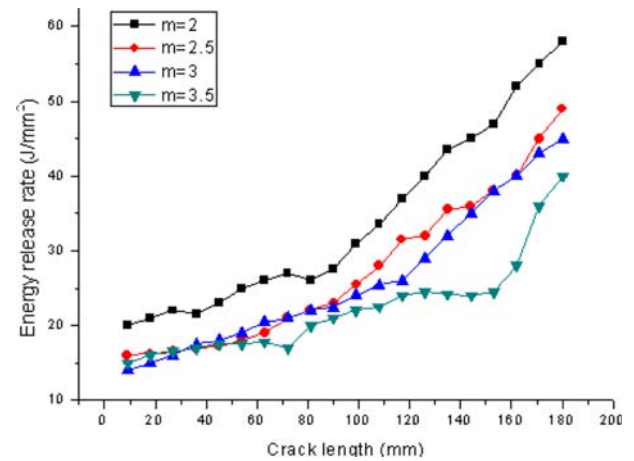


Fig. 8 G CBT graph depending on crack length

3. Test Result: Graph Showing Reaction Force Depending on Displacement

Fig. 7 is the graph indicating the axial displacement to crack length and comparison of the specimens. The displacement tends to increase in line with a developing crack. The displacement of the specimen with $m = 2$ appears to be the greatest. The lower the m value, the higher the displacement. This is attributable to the fact that the less the m value of specimen, the greater the bending force on beam.

Fig. 8 compares the energy release rate depending on the crack length of the specimen in the fatigue experiment. Energy release rate tends to increase in general while crack is developing. Energy release rate of the specimen with $m = 2$ appears to be the greatest, indicating 58 J/mm^2 . The lower the value of m , the higher the energy release rate, which is due to a greater effect of the load and the displacement of energy release rate.

4. Simulation to Verify the Experiment

To compare and verify the experimental result of the specimen with $m = 2$ through simulation, a model in the same dimension is designed.

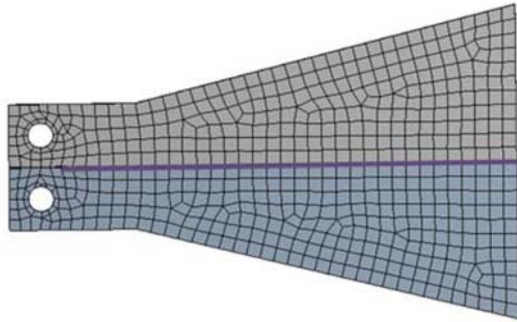


Fig. 9 Finite element model

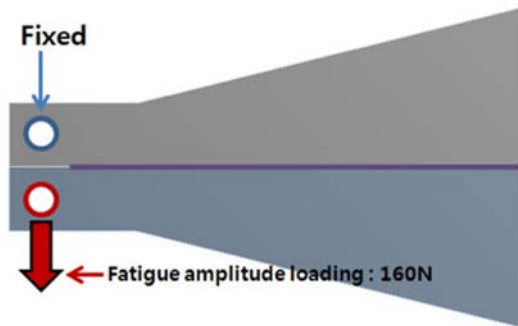


Fig. 10 Boundary condition of simulation

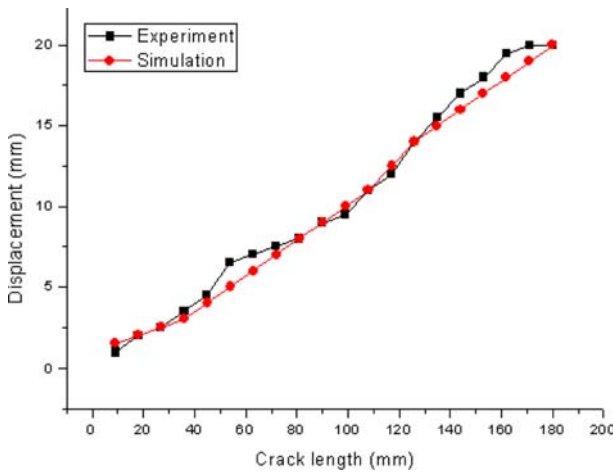


Fig. 11 Displacement graph depending on crack length (m = 2)

To save time for modeling and analysis, the model is designed with 2D and a finite element division is performed as in Fig. 9. The boundary condition of simulation is shown in Fig. 10. The pinhole of the loading block on top is fixed while the downward displacement condition is given to the pinhole of the loading block at the bottom.

Fig. 11 shows the displacement curve to crack length obtained as the result of fatigue experiment and simulation analysis of the TDCB specimen using aluminum foam, which compare the specimen with $m = 2$. Graphs are similar with each other in pattern and in general while experimental value is slightly higher than simulation analysis.

Fig. 12 is the G CBT curve depending on the crack length obtained from the fatigue experiment and simulation analysis of the TDCB specimen using aluminum foam which is compared to the specimen

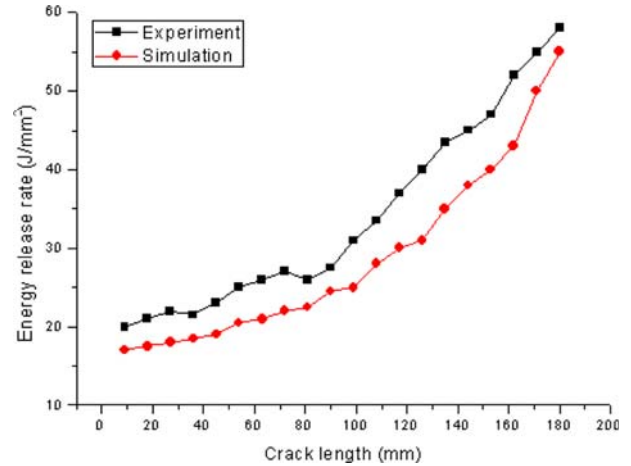
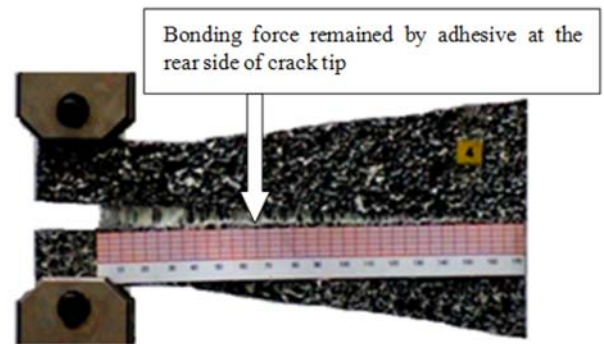
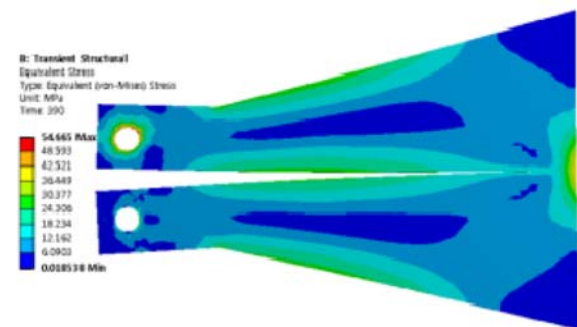


Fig. 12 G CBT graph (m = 2) depending on crack length



(a) Experimental configuration



(b) Analysis configuration

Fig. 13 Experimental and analysis configurations at the crack length of 150 mm (m = 2)

with $m = 2$. According to both experiment and analysis, in a low energy release rate at early stage of crack, energy release rate begins to increase in line with a developing crack. The maximum energy release rate is 55 J/mm^2 which is of a similar level. Generally, energy release rate from the experiment is higher by bonding strength which is maintained even after the specimen is separated.

Fig. 13 shows experimental and simulation configuration at the crack length of 150 mm ($m = 2$). Two figures are similar each other. As configurations of displacements at experiment and analysis are visibly similar at Figs. 13(a) and (b), simulation and experimental results approach each other at Fig. 11. As shown by Fig. 13(a) of experiment, the bonding force remained by adhesive influences energy release rate

at the rear side of crack tip during crack propagation by comparing with simulation result. Therefore, Fig. 12. shows the deviation between fatigue experiment and simulation analysis with similar trend.

5. Conclusion

As a result of testing the fatigue behavior of TDCB specimen glued using aluminum foam composite material, the following conclusion is made.

1. According to the analysis of axial displacement to crack length, displacement tends to increase in line with a developing crack and the displacement of the specimen with $m = 2$ appears to be the greatest. The lower the value of m , the greater the displacement, which is attributable to the fact that the lower the specimen's m value is, the greater the bending force on beam.

2. As regards the graph showing energy release rate to crack length, energy release rate tends to increase in line with a developing crack and the specimen with an energy release rate of $m = 2$ appears to be the greatest, indicating that the maximum energy release rate is 58 J/mm^2 and that the lower the m value of the specimen is, the greater its energy release rate. This is attributable to the greater effect of the load and displacement on energy release rate.

3. As a result of designing and analyzing the TDCB model under the same condition as the experiment, fatigue behavior among the layers could be similarly predicted.

4. Based on correlations obtained in this study, fatigue behavior of bonding material would possibly be analyzed and the aluminum foam material bonded using adhesive would be applied to a composite structure in various fields, thereby analyzing the mechanical and fracture characteristic of the material.

ACKNOWLEDGEMENT

This research was supported by Basic Science Research Program through the National Research Foundation of Korea (NRF) funded by the Ministry of Education, Science, and Technology (2011-0006548).

REFERENCES

- Pirondi, A. and Nicoletto, G., "Fatigue crack growth in bonded DCB specimens," *Engineering Fracture Mechanics*, Vol. 71, No. 4-6, pp. 859-871, 2004.
- Shokrieh, M. M., Heidari-Rarani, M., and Rahimi, S., "Influence of curved delamination front on toughness of multidirectional DCB specimens," *Composite Structures*, Vol. 94, No. 4, pp. 1359-1365, 2012.
- Blackman, B. R. K., Dear, J. P., Kinloch, A. J., MacGillivray, H., Wang, Y., Williams, J. G., and Yayla, P., "The failure of fibre composites and adhesively bonded fibre composites under high rates of test," *Journal of Materials Science*, Vol. 31, No. 17, pp. 4467-4477, 1996.
- Pradeep, K. R., Nageswara Rao, B., Srinivasan, S. M., and Balasubramaniam, K., "Interface fracture assessment on honeycomb sandwich composite DCB specimens," *Engineering Fracture Mechanics*, Vol. 93, No. 0, pp. 108-118, 2012.
- Marzi, S., Biel, A., and Stigh, U., "On experimental methods to investigate the effect of layer thickness on the fracture behavior of adhesively bonded joints," *International Journal of Adhesion and Adhesives*, Vol. 31, No. 8, pp. 840-850, 2011.
- Qiao, P., Wang, J., and Davalos, J. F., "Tapered beam on elastic foundation model for compliance rate change of TDCB specimen," *Engineering Fracture Mechanics*, Vol. 70, No. 2, pp. 339-353, 2003.
- Cho, J. U., Kinloch, A., Blackman, B., Rodriguez, S., Cho, C. D., and Lee, S. K., "Fracture behaviour of adhesively-bonded composite materials under impact loading," *Int. J. Precis. Eng. Manuf.*, Vol. 11, No. 1, pp. 89-95, 2010.
- Cooper, V., Ivankovic, A., Karac, A., McAuliffe, D., and Murphy, N., "Effects of bond gap thickness on the fracture of nano-toughened epoxy adhesive joints," *Polymer*, Vol. 53, No. 24, pp. 5540-5553, 2012.
- Michailidis, N., Stergioudi, F., Omar, H., and Tsipas, D. N., "An image-based reconstruction of the 3D geometry of an Al open-cell foam and FEM modeling of the material response," *Mechanics of Materials*, Vol. 42, No. 2, pp. 142-147, 2010.
- Wang, H., Yang, D., He, S., and He, D., "Fabrication of open-cell Al foam core sandwich by vibration aided liquid phase bonding method and its mechanical properties," *Journal of Materials Science & Technology*, Vol. 26, No. 5, pp. 423-428, 2010.
- BS 7991, "Determination of the Mode I Adhesive Fracture Energy GIC of Structure Adhesives Using the Double Cantilever Beam (DBC) and Tapered Double Cantilever Beam (TDCB) Specimens," 2001.
- Liu, J. A., Yu, S. R., Hu, Z. Q., Liu, Y. H., and Zhu, X. Y., "Deformation and energy absorption characteristic of $\text{Al}_2\text{O}_3/\text{Zn-Al}$ composite foams during compression," *Journal of Alloys and Compounds*, Vol. 506, No. 2, pp. 620-625, 2010.
- ISO 11343, "Adhesives-Determination of dynamic resistance to cleavage of high strength adhesive bonds under impact conditions-Wedge impact method," 1993.
- Raju, P., Rajesh, S., Satyanarayana, B., and Ramji, K., "Evaluation of stress life of aluminum alloy using reliability based approach," *Int. J. Precis. Eng. Manuf.*, Vol. 13, No. 3, pp. 395-400, 2012.
- Hur, J. W., "An experimental study on fatigue safety life assessment of aircraft engine support structure," *Int. J. Precis. Eng. Manuf.*, Vol. 12, No. 5, pp. 843-848, 2011.